Journal of Materials Chemistry A

Drastic Enhancement of Carbon Dioxide Adsorption in Fluoroalkyl-Modified Poly(allylamine)

Journal:	*Journal of Materials Chemistry A*
Manuscript ID	TA-ART-01-2021-000879.R1
Article Type:	Paper
Date Submitted by the Author:	20-Mar-2021
Complete List of Authors:	Koutsianos, Athanasios; Swansea University, Energy Safety Research Institute Hamdy, Louise; Swansea University, Department of Engineering; Swansea University Yoo, Chun-Jae; Georgia Institute of Technology, Lee, Jason ; Georgia Institute of Technology Taddei, Marco; Università degli Studi di Pisa, Department of Chemistry and Industrial Chemistry Urban-Klaehn, Jagoda ; Idaho National Laboratory Dryzek, Jerzy ; Polish Academy of Sciences, Institute of Nuclear Physics Jones, Christopher; Georgia Institute of Technology, Chemical and Biomolecular Engineering Barron, Andrew; Swansea, ESRI Andreoli, Enrico; Swansea University, Engineering

Drastic Enhancement of Carbon Dioxide Adsorption in Fluoroalkyl-Modified Poly(allylamine)

*Athanasios Koutsianos,[a,†] Louise B. Hamdy,[a] Chun-Jae Yoo,[b] Jason J. Lee,[b] Marco Taddei,[a,‡] Jagoda M. Urban-Klaehn,[c] Jerzy Dryzek,[d] Christopher W. Jones,[b] Andrew R. Barron,[a,e,f] and Enrico Andreoli[a]**

[a] *Energy Safety Research Institute, Swansea University, Bay Campus, Swansea, SA1 8EN, UK*

[b] *School of Chemical & Biomolecular Engineering, Georgia Institute of Technology, Atlanta, GA 30332, USA*

[c] *Energy and Environment S&T, Idaho National Laboratory, Idaho Falls, ID 83415, USA*

[d] *Institute of Nuclear Physics Polish Academy of Sciences, PL-31342 Krakow, Poland*

[e] *Department of Chemistry and Department of Materials Science and Nanoengineering, Rice University, Houston, TX 77005, USA*

[f] *Faculty of Engineering, Universiti Teknologi Brunei, Brunei Darussalam*

† Current Address: Anorganische Chemie, Fakultät für Chemie und Chemische Biologie, Technische Universität Dortmund, Otto-Hahn-Straße 6, 44227 Dortmund, Germany

‡ Current Address: Department of Chemistry and Industrial Chemistry, University of Pisa, Pisa 56124, Italy

**e.andreoli@swansea.ac.uk; +44(0)1792602524*

Abstract

Polyamine-based carbon dioxide sorbents suffer from a seesaw relationship between amine content and amine efficiency. High polyamine loadings equate to increased amine contents, but often at the expense of amine efficiency. Carbon dioxide mass transport in compact polymers is severely limited, especially at ambient temperature. High polymer contents curtail diffusion pathways, hindering CO_2 from reaching and reacting with the numerous amine functions. Here, we overcome this issue using poly(allylamine) (PAA) grafted with short fluoroalkyl chains and then cross-linked with C_{60}. As experimentally evidenced by positron annihilation lifetime spectroscopy, the incorporation of fluoroalkyl chains generates free volume elements that act as additional diffusion pathways within the material. The inclusion of void volume in fluoroalkyl-functionalized PAA sorbents results in radically increased CO_2 uptakes and amine efficiencies in diluted gas streams at room temperature, including simulated air. We speculate that the hydrophobic fluorinated functions interfere with the strong amine hydrogen bonding network disrupting and consequently altering the packing and conformation of the polymer chains. The evidence presented here is a blueprint for the development of more efficient amine-based CO_2 sorbents.

Introduction

Global warming and climate change are directly linked to CO_2 emissions from fossil fuels combustion. Since 1958, the National Oceanic and Atmospheric Administration has been recording the continuous rise in atmospheric CO_2 concentration reaching today 417 ppm.[1] With a mean average growth of about 2.6 ppm per year in the last five years, we are set to witness a record concentration of 500 ppm by 2050. In the face of such a looming

perspective, many countries keep relying on fossil fuels as a primary energy source, while we transition to a net-zero-carbon society.[2] Consequently, remedies are sought to prevent the further release of CO_2 and enable its removal from the atmosphere. The deployment of carbon capture and storage (CCS) technologies at scale is seen by many as the solution to implement the transition to net-zero emissions. Aqueous amine scrubbing, originally developed in the 1930s to remove CO_2 from natural gas, is acknowledged as the benchmark technology for the removal of CO_2 from power plant flue gases,[3, 4] yet it suffers from limited capture capacity, high energy demand, and continuous replenishing of corrosive amines.[5] Nowadays, however, it is clear that decarbonizing power plants, industrial activities, transport, and heating are not sufficient measures to avoid the environmental impact of climate change. Responding to the mounting urgency of reducing atmospheric CO_2 concentrations, researchers are increasingly looking towards the development of materials suitable for the capture of CO_2 from the air, the concept of direct air capture (DAC).[6, 7] This presents new challenges to carbon capture technologies, not least in the highly diluted nature of the CO_2 adsorbate at only around 400 ppm, compared to more concentrated CO_2 sources such as flue gas (12-15% CO_2).[8] In the last decade, there has been a growing and sustained effort to develop carbon capture technologies for large-scale application, including CO_2 capture with solid sorbents as an alternative to amine scrubbing.[9] Development and optimization of the chemistry and physics of sorbent materials are key steps for the technical feasibility of efficient CO_2 capture from flue gas or air. A recent tutorial review suggests six pillars for the optimum design of the sorbent materials, namely capacity, selectivity, thermal and chemical stability, recyclability, low cost, and fast kinetics.[8] Among these factors, the majority of the studies have been directed

towards the development of materials with higher capacity, increased selectivity and stability to impurities.

Supported polyamine-based sorbents have attracted increased attention as promising candidates for DAC due to their high performance and stability.[10, 11] Additionally, their adsorption performance is often enhanced by the presence of water,[12-14] a useful feature for adsorbents that would invariably be exposed to some levels of humidity.[15-18] The loading of as much amine as possible has initially been the objective of solid sorbent development, as two amines are needed to bind one CO_2 molecule for the formation of ammonium carbamate pairs, among other related species, in dry gaseous streams.[19] However, thermodynamic and kinetic factors act competitively in the sorption process,[20] and it has been evident that high amine loadings often counteract gas diffusion in the bulk, reducing the CO_2 adsorption working capacity. Nonetheless, at higher adsorption temperatures, diffusion may be enhanced to achieve higher CO_2 uptakes.[21] Although this may aid post-combustion CO_2 adsorption, DAC conditions generally involve ambient temperatures, which for amine-based chemisorbents requires facilitated access to the amine groups. Thus, current studies aim to strike a successful trade-off between amine loading and accessibility to maximize amine efficiency, i.e., the moles of CO_2 adsorbed per mole of amine functions.

The main strategies to enhance CO_2 diffusion and amine efficiency in supported solid amine sorbents are (i) the structural modification of the support, (ii) the alteration of the interaction between aminopolymer and support, and (iii) the modification of the polymer itself. Various studies emphasize the structural features of the support and how they affect CO_2 uptake.[22-28] The combination of pore diameter, pore length, and residual pore volume

have been identified as the pivotal factors affecting polyamine loading, amine accessibility, and so the CO_2 uptake.[22-24, 27, 29]

It has also been reported that surface chemistry of the support has a major effect on adsorption behavior, and tuning the chemical properties can affect adsorption capacity.[30-33,34] Hydrophobic features have been incorporated onto silica to establish a repulsive interaction with PEI and expose more amine functionality. The synthesized sorbent exhibited both higher uptake and sorption rate due to the interaction of the host support with active amines such that the amines became more easily accessible.[35] Similarly, Sayari et al.[36, 37] observed increased amine efficiency in a PEI-based sorbent after doping the silica support with a surface layer of long hydrophobic alkyl chains. The improved efficiency was related to a better dispersion of PEI in the presence of the alkyl chains. In a previous study on an unsupported adsorbent, we provided evidence that the cross-linking of poly(propylenimine) (PPI) with hydrophobic fullerene diminished the enthalpic barrier of CO_2 capture whilst increasing the entropy of adsorption. We suggested that the repulsive interplay between hydrophobic C_{60} and hydrophilic amines better exposed the latter to CO_2.[38] Indeed, a separate computational study by Sharma et al.[39] revealed the significance of entropic contributions in CO_2 capture in a PEI melt. Entropically favorable free volume was identified as the dominant factor in the sorption process, as higher CO_2 solubility values were noticed near the interfaces despite the lower density in sorption sites.

Distinct from the aforementioned studies, several groups directly modified the active amine component with surfactant/diffusion additives to better disperse it onto the support and improve amine efficiency.[40-42] The observed enhancement was assigned to kinetic factors and was further corroborated by a decrease in the optimum sorption temperature after

surfactants addition. Morphology and conformational changes of the polymer after surfactant addition promoted the interaction between amines and CO_2. Additives can also increase thermal and oxidative stability of the sorbent.[43]

Driven by the above findings on the pivotal role of polymer conformation in the CO_2 capture process, and the beneficial effect of hydrophobicity functionality on amine accessibility, we present here the successful implementation of a strategy to improve the CO_2 capture performance at ambient temperature of unsupported, highly loaded poly(allylamine) (PAA) fullerene cross-linked sorbents. We demonstrate the creation of free void volume upon inclusion of hydrophobic fluoroalkyl short chains on the aminopolymer, resulting in a dramatic enhancement of both CO_2 capture capacity (2.8-fold increase) and amine efficiency (4.1-fold increase). Also, the inclusion of voids allowed achievement of a CO_2 uptake of 1.30 mmol/g in 400 ppm CO_2 at 30 °C, corresponding to a 3-fold increase compared to the unmodified sorbent.

Results and Discussion

A solution of PAA was obtained after treating poly(allylamine) hydrochloride in a methanolic solution of caustic alkali (KOH). The exact concentration of PAA present in the resulting solution was determined after solvent removal, as described in the experimental section. Fluoroalkyl groups were grafted to the PAA chains through a nucleophilic addition reaction with glycidyl 2,2,3,3,4,4,5,5-octafluoropentyl ether (GOF, chemical formula $C_8H_8F_8O_2$) at ambient temperature. Unmodified and GOF-functionalized PAA were subsequently cross-linked with $C_{60,}$ resulting in the formation of PAA-C_{60} and F-PAA-C_{60}, respectively (see reaction schematic in Figure 1). Scanning electron microscopy (SEM) images of the two materials are provided in Figure S1 of the Electronic

Supplementary Information (ESI). F-PAA-C_{60} with two different GOF loadings were prepared, F1-PAA-C_{60} and F2-PAA-C_{60}, with a higher level of fluoroalkyl functionalization in the latter (Table 1). Energy dispersive X-ray (EDX) spectroscopy was used to confirm the presence of fluorine in F-PAA-C_{60}, demonstrating the incorporation of fluoroalkyl groups in the material, see Figure S2 (see ESI). The ring-opening of the epoxide functional group was also confirmed using Fourier Transform Infrared (FTIR) spectroscopy. The FTIR spectrum of F1-PAA-C_{60} is shown in Figure 2. The peak at 1165 cm^{-1} is attributed to the C-O stretching of alcohols.[44] As expected, no such peak is observed in the spectrum of PAA-C_{60}. Detailed assignment of the peaks is provided in Figure S3 (see ESI). Finally, the hydrophobic nature of the GOF additive reduced the water uptake of F1-PAA-C_{60} compared to PAA-C_{60} (Figure S4).

The amounts of PAA, C_{60}, and GOF in the materials were determined from the elemental analyses of the vacuum dried samples, assuming all oxygen was solely due to the epoxy rings of the fluoroalkyl groups (Tables 1 & S1, see ESI). Detailed calculations are provided in the ESI. Clearly, PAA-C_{60} is a highly loaded polyamine-based material with 80.6 wt.% of its weight due to PAA, and only the remaining 19.4 wt.% to the cross-linker C_{60}. This compares to polymer loadings of about 70 wt.% in both poly(ethyleneimine) (PEI)-C_{60} and poly(propylenimine) (PPI)-C_{60} in our previous work.[38, 45] As displayed in Table 1, the PAA loading drops to about 60 wt.% with the inclusion of fluoroalkyl groups in F-PAA-C_{60}, and the cross-linker also drops to about 15 wt.%. The molar ratios of allylamine (AA) monomeric units, fullerene, and GOF were also calculated (Table S1). The AA:C_{60} molar ratio is about 50:1 (1:0.02) for all materials. It follows that in both PAA-C_{60} and F-PAA-C_{60} there are about 150 polymer carbons per fullerene (since each AA contains 3 carbons).

This compares to 120 and 100 polymer carbons per fullerene in PEI-C_{60} and PPI-C_{60}, respectively.[38, 45] It appears that the higher polymer loading of PAA-C_{60} and F-PAA-C_{60} also corresponds to the largest amount of added carbon per fullerene unit. Thus, it cannot be naturally predicted that PAA-C_{60} would achieve CO_2 capture capacities (g of CO_2 captured per g of material) higher than PEI-C_{60} and PPI-C_{60}, given the more significant amount of carbon present in the sorbent. Even more so in the case of F-PAA-C_{60}, where the fluoroalkyl chains add almost 30 wt.% extra weight to the sorbent material, corresponding to about one GOF grafted for every 10-12 amines (Table 1). Astonishingly, as demonstrated later in the paper, F-PAA-C_{60} can absorb almost as much CO_2 as PAA-C_{60} at its optimum sorption temperature, despite the lower amine content per unit of weight, indicating the beneficial impact of the fluoroalkyl groups to enhance amine efficiency.

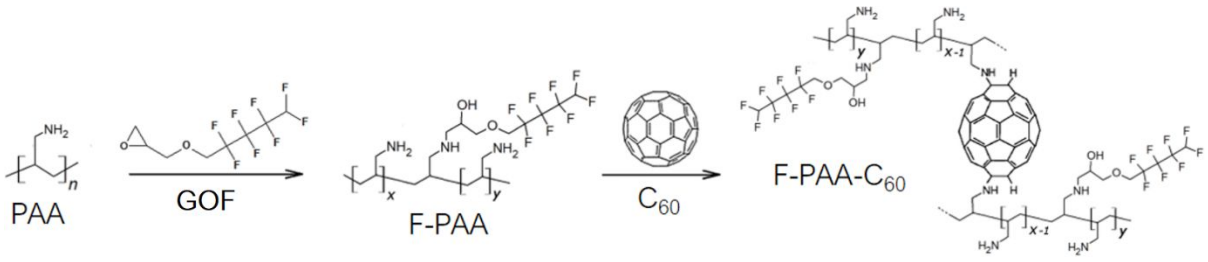

Figure 1. Synthetic route for the grafting of PAA with fluorinated additive GOF to give partially fluorinated F-PAA, and its reaction with fullerene C_{60} to form F-PAA-C_{60}.

Table 1. Chemical composition of the vacuum dried samples according to elemental analysis

Sample	PAA (wt.%)	C_{60} (wt.%)	GOF (wt.%)	Molar ratios
PAA-C_{60}	80.5	19.5	-	$(AA)_1$ $(C_{60})_{0.019}$
F1-PAA-C_{60}	61.3	15.2	23.4	$(AA)_1$ $(C_{60})_{0.020}$ $(GOF)_{0.075}$
F2-PAA-C_{60}	57.0	13.9	29.1	$(AA)_1$ $(C_{60})_{0.020}$ $(GOF)_{0.101}$

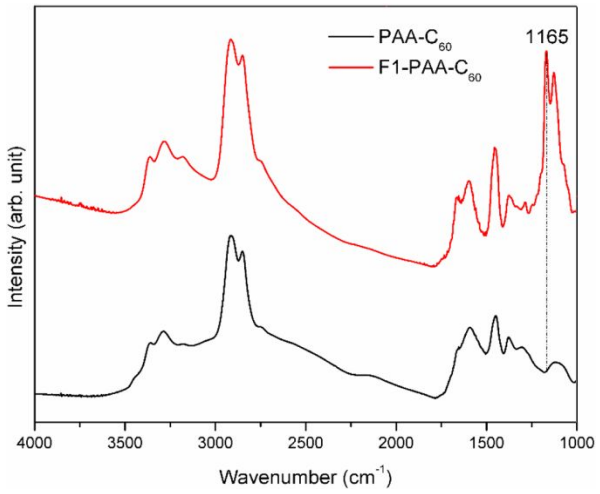

Figure 2. FTIR spectra of PAA-C_{60} and F1-PAA-C_{60}. Prior to analysis the materials were vacuum-dried at 90 °C. Full peak assignments are given in Figure S3 (see ESI).

Carbon Dioxide Capture

A major difference between PAA-C_{60} and its fluoroalkyl-modified versions is the effect of temperature on CO_2 uptake. Figure 3 shows the CO_2 gravimetric equilibrium uptakes of PAA-C_{60}, F1-PAA-C_{60}, and F2-PAA-C_{60} in pure CO_2 (the gravimetric curves corresponding to each data point are provided in Figure S5, see ESI). The gravimetric curve of plain PAA is also provided in Figure S6, highlighting the inability of the CO_2 to interact

with the amine functions of the unmodified polymer. Clearly, PAA-C_{60} is a poorer sorbent than F-PAA-C_{60} at a lower temperature. The CO_2 uptake of PAA-C_{60} decreases with decreasing temperature, whereas the uptake of both F1-PAA-C_{60} and F2-PAA-C_{60} improves at a lower temperature (similar trends were observed in 10% CO_2, as shown in Figure S7, see ESI). This is a fundamental change in the behavior of the material, highlighting the striking effect of the fluoroalkyl groups on the availability of the polymer amino groups towards CO_2 capture. In Figure 3a, the uptake of PAA-C_{60} drops from 0.191 to 0.065 g/g at 90 and 30 °C, respectively, evidently losing access to 2/3 of its amine functionalities at low temperature. Instead, the capacity of F1-PAA-C_{60} increases from 0.120 to 0.143 g/g, almost independent of the change in temperature. This is further enhanced when more fluoroalkyl groups are present in the materials since the capture capacity of F2-PAA-C_{60} improves from 0.143 to 0.178 g/g at 90 and 30 °C, respectively.

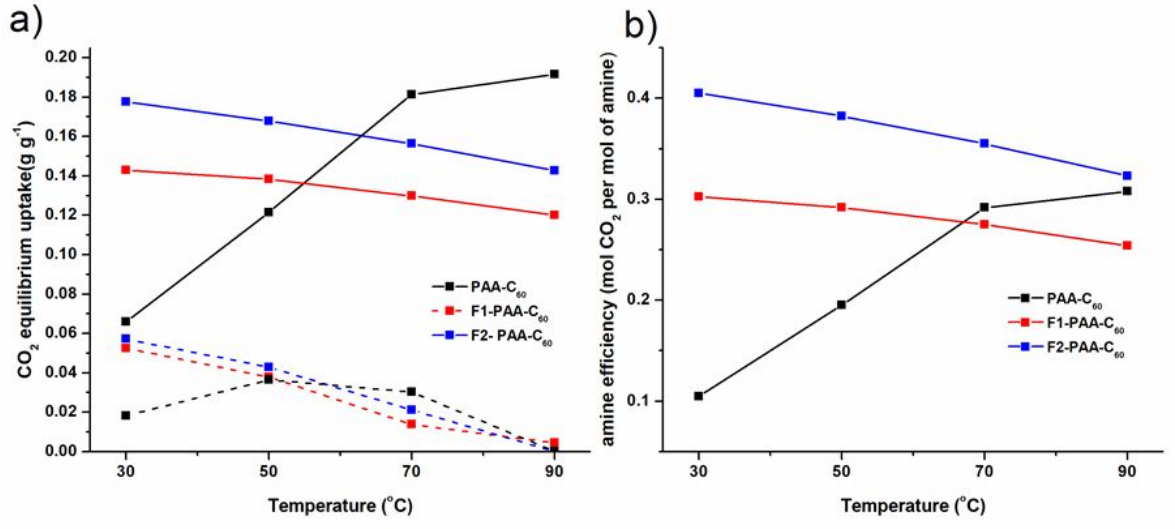

Figure 3. a) CO_2 uptake vs temperature for PAA-C_{60} (black), F1-PAA-C_{60} (red) and F2-PAA-C_{60} (blue) in 100% CO_2 (solid lines) or 400 ppm CO_2 in N_2 (dashed lines); b) amine efficiency in 100% CO_2 as a function of temperature, PAA-C_{60} (black), F1-PAA-C_{60} (red) and F2-PAA-C_{60} (blue).

The maximum CO_2 sorption capacity of PAA-C_{60} is achieved at 90 °C, the highest useful temperature, since material degradation and performance loss are observed above 90 °C. Increased temperature in the high polyamine loaded PAA-C_{60} (80.5 wt.% PAA) enhances the motion and dynamics of polymer chains, alleviating the diffusion hindrance and allowing the penetration of gaseous CO_2 in the bulk of the material.[42] On the contrary, an uptake of just 0.065 g/g at 30 °C clearly indicates the kinetic inhibition of CO_2 diffusion at this temperature. The addition of GOF drastically changes this behavior, with F1-PAA-C_{60} taking up to 2.2 times more CO_2 than PAA-C_{60} at 30 °C. This is striking considering the significantly lower polymer content of F1-PAA-C_{60} (61.3 wt.% PAA) compared to PAA-C_{60}. A better way to picture the dramatic difference of polymer performance in the two materials is to normalise the CO_2 capture capacity per weight of PAA, the sorptive component. It follows that the polymer in PAA-C_{60} captures 0.081 g CO_2 per gram of PAA, while in F1-PAA-C_{60} it captures 0.233 g CO_2 per gram of PAA at 30 °C. Evidently, the presence of fluoroalkyl groups is beneficial for CO_2 capture at a lower temperature. Even more pronounced is the effect observed for F2-PAA-C_{60} (57.0 wt.% PAA), with a CO_2 uptake of 0.178 g/g at 30 °C, an increase of 2.74 times the capacity compared to PAA-C_{60} despite having almost 1/3 less polymer in the material. This corresponds to 0.312 g CO_2 captured per gram of PAA present in F2-PAA-C_{60}. This high performance is consistent across all the investigated temperature range. The slight decrease of CO_2 capture capacity at higher temperature can be associated with weakly bound CO_2 in both F1-PAA-C_{60} and F2-PAA-C_{60} that can only be adsorbed at a lower temperature. It is also of note, the cyclability displayed by F-PAA-C_{60} materials. The stability was investigated for 23 consecutive adsorption-desorption cycles (adsorption: 100% CO_2, at 25 °C; desorption:

100% Ar at 90 °C). The CO_2 adsorption-desorption profiles and the relevant CO_2 working capacities are shown in Figure S8 (see ESI). After 23 cycles, the working capacity of the GOF functionalized material dropped from 0.088 g/g to a substantially steady value of 0.074 g/g after the first few cycles.

A comparison of amine efficiency (mol of CO_2 uptake per mol of amine) between PAA-C_{60} and F-PAA-C_{60} confirms the CO_2 capture enhancing effect of the fluoroalkyl additive. In Figure 3b, the amine efficiency of PAA-C_{60} is highest at a higher temperature, 0.31 mol/mol at 90 °C (1 CO_2 every 3.3 amines), and lowest at a lower temperature, 0.10 mol/mol at 30 °C (1 CO_2 every 10 amines), corresponding to a dramatic loss of bulk amine accessibility. This inaccessibility is entirely overcome in the presence of GOF. The amine efficiency of F1-PAA-C_{60} and F2-PAA-C_{60} are 3 and 4 times higher than that of PAA-C_{60} at 30 °C, respectively. The outstanding performance of F2-PAA-C_{60} deserves to be highlighted with a value of 0.41 mol CO_2/mol NH_2, approaching the theoretical maximum ratio of one CO_2 molecule captured every two amine groups in dry conditions (ammonium carbamate pathway).[46] These performances have been recorded in pure CO_2, however the enhanced amine availability in F-PAA-C_{60} is expected to boost the CO_2 uptake in diluted gas streams too.

Indeed, simulated direct air capture (DAC) from a stream of 400 ppm CO_2 in nitrogen further highlights the difference in performance between PAA-C_{60} and F-PAA-C_{60}. In Figure 3a, all materials display a low DAC uptake at 90 °C (dashed lines); nonetheless, the performance significantly improves at a lower temperature (the gravimetric curves corresponding to each data point are provided in Figure S4, see ESI). The DAC capacity of PAA-C_{60} goes through a maximum with the highest uptake of 0.036 g/g measured at 50

°C; the uptake drops to 0.019 g/g at 30 °C. Instead, the GOF-functionalized materials show the best performance at 30 °C. At this temperature, F1-PAA-C_{60} and F2-PAA-C_{60} capture 0.053 and 0.057 g/g, respectively, demonstrating high CO_2-philicity essential for DAC applications. The fluoroalkyl groups in F-PAA-C_{60} triple the DAC capacity of PAA-C_{60} at low temperature, in line with the fourfold increase of CO_2 uptake observed in a pure CO_2 stream. With a DAC capacity of 1.30 mmol/g (2.28 mmol CO_2 per gram of PAA) at 30 °C, F-PAA-C_{60} compares well with other materials reported in the literature such as PEI loaded SBA-15 (1.10 mmol/g),[47] PEHA or TEPA co-impregnated with PO on silica support (1.25 and 1.34 mmol/g, respectively),[43] and amine-based nanofibrillated cellulose (1.39 mmol/g).[48] A comprehensive table with key features and performance of polyamine-based DAC sorbent materials is provided in the SI, Table S2. The highest DAC capacity recorded to date is 3.36 mmol/g in a humidified stream of 400 ppm CO_2, Jones and co-workers achieved this outstanding performance using a bimodal meso/macroporous hierarchical silica impregnated with PEI.[29]

Single component CO_2 adsorption isotherms also demonstrate the ability of PAA-C_{60} and F-PAA-C_{60} to capture CO_2 at low pressure, as shown in Figure 4. At 0.07 bar, mimicking performance in diluted gas streams, PAA-C_{60} and F1-PAA-C_{60} adsorb 0.026 g/g and 0.104 g/g at 25 °C, respectively (inset of Figure 4a). This is again a 4-fold increase of CO_2 capture capacity upon introduction of fluoroalkyl groups in the material, in agreement with the gravimetric measurements. At 1 bar and 25 °C, the CO_2 uptakes are 0.050 and 0.150 g/g for PAA-C_{60} and F1-PAA-C_{60}, respectively. Further increasing the pressure results only in a slight improvement of CO_2 capture, evidence of the limited effect of pressure on the accessibility of bulk amino groups. In the case of PAA-C_{60}, the bulk amino groups become

accessible when the temperature is increased to 90 °C, reaching an uptake of 0.208 g/g at 5 bar. This is not observed for F1-PAA-C_{60}, where the CO_2 capture capacity is lower at a higher temperature, i.e. 0.122 g/g at 90 °C instead of 0.177 g/g at 25 °C and 5 bar. This shows that at 90 °C the interaction of CO_2 is stronger with PAA-C_{60} than with F1-PAA-C_{60} since more thermal energy weakens the CO_2-amine interaction only in the presence of fluoroalkyl groups. Supporting evidence to this observation is given later, where the isosteric heat of CO_2 adsorption is greater for PAA-C_{60} (110 KJ/mol) than F1-PAA-C_{60} (70 kJ/mol) for a CO_2 loading of about 0.080 g/g at 90 °C.

A comparison of the CO_2 sorption kinetics of PAA-C_{60} and F1-PAA-C_{60} is provided in Figure 4. The plot in Figure 4b shows the amount of CO_2 adsorbed by each sorbent upon the addition of a first dose of CO_2, starting with the materials in a vacuum at either 25 or 90 °C. The uptakes reach their plateaus once the materials are fully saturated with CO_2 (corresponding to a rate of pressure drop of less than 0.01 mbar/min). Likewise, Figure 4c shows the uptakes upon the addition of a second dose of CO_2, starting from the equilibrium conditions of the first dose. Figure 4d is a summary of the equilibrium uptakes, times required to reach equilibrium, and equilibrium pressures achieved by each material after the first and second dose of CO_2 at 25 and 90 °C, respectively (made from the data presented in Figures 4a, b, and c). Focusing on the data collected after the first dose, it is evident that there is no major difference between the CO_2 sorption performance of PAA-C_{60} and F1-PAA-C_{60} at both 25 and 90 °C. Both materials achieved similar uptakes (8 and 9 mg/g, at 25 °C, and 10 and 7 mg/g, at 90 °C, for each material respectively) within comparable times (11 and 4 min for both materials at 25 and 90 °C, respectively) and final equilibrium pressures (0.7 and 0.3 mbar, at 25 °C, and 1 and 1.5 mbar,

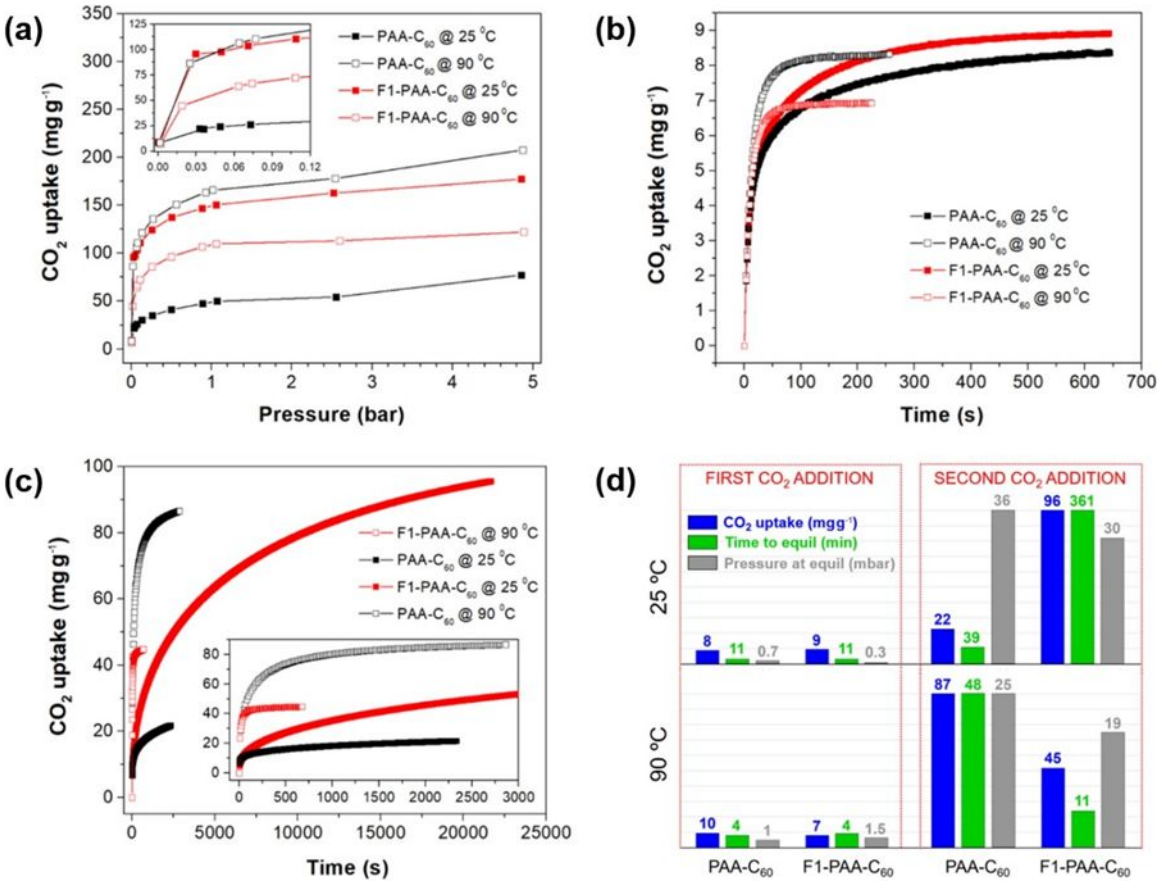

Figure 4. a) CO_2 adsorption isotherms of PAA-C_{60} (black) and F1-PAA-C_{60} (red) at 25 °C (filled symbols) and 90 °C (empty symbols). b) Kinetics of CO_2 uptake after exposure of the sorbents to a first dose of CO_2 for PAA-C_{60} (black) and F1-PAA-C_{60} (red) at 25 °C (filled symbols) and 90 °C (empty symbols). c) The same of b) but for a second dose of CO_2. d) CO_2 uptake (mg/g, colored in blue), time to (min, colored in green) and pressure at (mbar, colored in grey) equilibrium for PAA-C_{60} and F1-PAA-C_{60} after the first and second dose of CO_2 at 25 and 90 °C (the exact values are shown on the top of the bars; for each parameter, the height of the bars is normalised against the highest value).

at 90 °C, for each material respectively). It is only after the second dose that the different CO_2 sorption behavior of the two materials becomes evident. At 25 °C, F1-PAA-C_{60}

adsorbed 96 mg/g of CO_2 compared to just 22 mg/g for PAA-C_{60}, highlighting the better low-temperature accessibility of amino groups in the fluoroalkyl-modified sorbent. However, it is also relevant to note that the kinetics of sorption in F1-PAA-C_{60} is slow since it took 361 min (6 hours) for equilibrium to be reached with a final pressure of 30 mbar CO_2. The opposite situation was observed at 90 °C since it was PAA-C_{60} to adsorb 87 mg/g of CO_2 instead of F1-PAA-C_{60} with 45 mg/g after the second dose of CO_2 (Figure 4c). Clearly, the incorporation of fluoroalkyl additive in the sorbent facilitates the CO_2 transport in the sorbent. It is anticipated that these results should apply to alternative cross-linkers cheaper than C_{60}, as demonstrated in previous work with epoxy resin bisphenol-A diglycidyl ether (D.E.R. 332),[14] supporting the development of a new class of CO_2 capture materials for large-scale applications.

Microcalorimetry

The enhanced CO_2 sorption performance of the fluoroalkyl-modified adsorbents at low temperature prompted us to further investigate the amine-CO_2 interaction by measuring the heat of adsorption (Qst). In the literature, isosteric heat of adsorption values are often obtained by applying the Clausius-Clapeyron equation to models fitted to multiple adsorption isotherms collected at various temperatures.[14, 49] A more accurate method of measurement is to determine the Qst values directly via microcalorimetry,[50] as it was previously shown that the former method can be prone to erroneous results, when comparing the Qst values for aminosilica materials obtained via both techniques.[51, 52] For this study, we used a Tian-Calvet calorimeter to measure the heat released during the interaction of PAA-C_{60} and F1-PAA-C_{60} with CO_2 at incremental pressures, providing the energetics of CO_2 binding for both materials. The CO_2 uptakes shown in Figure 5a are in very good agreement with those previously presented in Figure 4a (see inset). It is worth

noting that only for PAA-C_{60}, the amount of CO_2 captured at 25 °C (Figure 4a) is about half of that adsorbed at 30 °C (Figure 5a); evidence of the strong temperature dependence of CO_2 mass transport in the sorbent without fluoroalkyl modification. Figure 5b is a plot of the Qst values measured in relation to the CO_2 uptakes. At near-zero CO_2 coverage (ca. 3 mg/g), the Qst values lay between 99 and 115 kJ/mol at both 30 and 90 °C for both PAA-C_{60} and F1-PAA-C_{60}, values typically observed for chemisorption, i.e., for chemical reactions between CO_2 and the amino groups of the sorbent material.[53] This is close to the value of 93 kJ/mol at adsorption of 0.03 mmol CO_2/g (1.32 mg/g) for PEI-impregnated SBA-15,[50] and 98 kJ/mol for zero CO_2 coverage on 3-amino-propyltriethoxysilane-functionalized MCM-41 silica,[54] both measured at 30 °C via microcalorimetry. Similarly, high Qst values at low loadings have been reported for polyaldehyde phosphorous dendrimer cross-linked PEI (103 kJ/mol),[55] and triamine surface-modified pore-expanded-MCM-41 (> 90 kJ/mol).[56] High Qst values were attributed to high amine loading and the proximity of available amine sites to form alkyl ammonium carbamate species upon adsorption of CO_2.[50] At low CO_2 coverage, it appears that the Qst values at 30 °C are roughly 5-15 kJ/mol lower than those measured at 90 °C, for F1-PAA-C_{60} and PAA-C_{60}, respectively, showing a slight dependence of the heat of CO_2 sorption on temperature, which is most significant for PAA-C_{60}.

The heat of adsorption of PAA-C_{60} is strongly dependent on CO_2 sorption temperature (Figure 5). At 30 °C, the Qst values drop sharply with increased CO_2 loading. In going from ca. 3 to 44 mg/g CO_2 uptake, the heat of sorption drops drastically from 99 kJ/mol, strongly indicative of chemisorption, to 13 kJ/mol, below the boundary for physisorption interactions.[8]

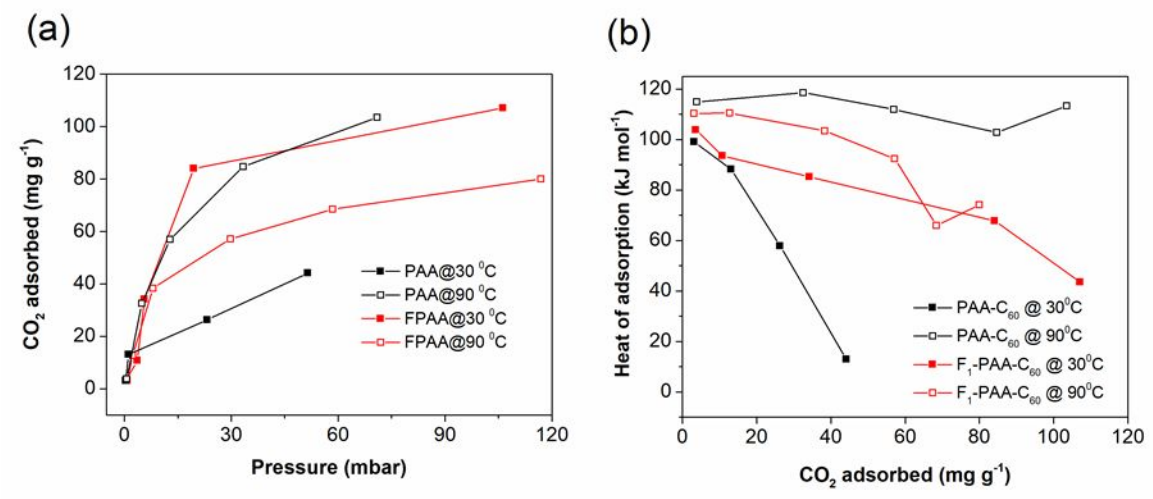

Figure 5. a) CO_2 uptake and b) isosteric heat of adsorption of PAA-C_{60} (black) and F1-PAA-C_{60} (red) measured at 30 °C (filled symbols) and 90 °C (empty symbols).

As discussed, PAA-C_{60} is affected by substantial CO_2 diffusion limitations at 30 °C, therefore, at low loadings (up to 10 mg/g), CO_2 can chemisorb only on the most accessible amine sites present on the surface of the material. This is in line with the two-site adsorption behavior described by Serna-Guerrero et al.,[57] in which once the outermost amines are saturated with chemisorbed CO_2 at low initial pressures, additional CO_2 can only be captured through weak physical interactions resulting in low heats of adsorption – less than 20 kJ/mol for CO_2 loadings above 40 mg/g for PAA-C_{60}. Most of the amines within the bulk of PAA-C_{60} are not accessible at 30 °C, resulting in low CO_2 adsorption, and the presence of strong electrostatic interactions among any surface alkyl ammonium carbamate species is likely to obstruct this access further.[29] This obstruction is overcome at 90 °C, when CO_2 diffusion into the bulk of the material, and subsequent CO_2 adsorption, is greatly enhanced. This is evidenced in that, at 90 °C, the Qst values are above 100 kJ/mol at all

investigated CO_2 loadings, up to above 100 mg/g. This demonstrates that temperature has a major effect on the accessibility of amines in PAA-C_{60}.

The heat of adsorption of F1-PAA-C_{60} is substantially less affected by the CO_2 sorption temperature (Figure 5b). At both 30 and 90 °C, the Qst of F1-PAA-C_{60} decreases with increasing CO_2 coverage, with the two trends laying between those of PAA-C_{60} recorded at the two temperatures. The Qst values diminish about linearly from ca. 110 to 40 kJ/mol in going from ca. 3 to 105 mg/mol, respectively. It has been observed that the fluorinated additive of F-PAA-C_{60} raises CO_2 adsorption capacity at 30 °C (Figure 5a) and influences the adsorbent CO_2 uptakes and amine efficiencies (Figure 3b), such that they are more consistent across the investigated range of temperatures in comparison to PAA-C_{60}. In Figure 5b it can be seen that, at 30 °C, the inclusion of the fluoroalkyl additive raises the Qst values of F-PAA-C_{60}, bringing about a similar effect on the Qst values at comparable CO_2 loadings as does increasing the temperature of adsorption for PAA-C_{60} to 90 °C. This is due to the greater diffusivity that the F-PAA-C_{60} allows for CO_2, enabling the formation of more ammonium carbamate species and higher adsorption capacity. At 90 °C, the Qst values of F-PAA-C_{60} are lower than PAA-C_{60} at similar CO_2 loadings. Higher Qst values are observed for adsorbents of higher amine density.[51] The disruptive effect of the fluoroalkyl chains of F-PAA-C_{60} may result in a higher incidence of isolated amines that are prevented from forming ammonium carbamate species with a neighboring amine. Instead, they form more of the less stable carbamic acid, which has a lower heat of adsorption,[47] and reduced uptakes of CO_2 are observed. This is entirely in line with our previous work on poly(propylenimine) (PPI) cross-linked C_{60}, where increasing hydrophobicity reduced the overall activation energy barrier for adsorption.[38]

In-situ Transmission FTIR Spectroscopy

The chemical species formed upon CO_2 adsorption on PAA-C_{60} and F1-PAA-C_{60} were investigated using *in-situ* FTIR in dry CO_2. In line with the previous measurements, two temperatures were investigated, namely 30 and 90 °C. Interestingly, no considerable differences were observed in the FTIR spectra recorded at the two temperatures for each material (Figures 6 & S9, see ESI). Evidence of CO_2 adsorption species should appear with peaks in the region between 1800 and 1300 cm^{-1}. In Figure 6, the peak at 1690 cm^{-1} is assigned to the C=O stretching of carbamic acid;[58, 59] this peak is more intense in F1-PAA-C_{60}, possibly due to the presence of hydroxyl group in the material after epoxide addition and its capability to stabilize carbamic acid.[6060] Likewise, the shoulder at 1400 cm^{-1} is related to the OH bending vibration of carbamic acid, which is also more prominent in the case F1-PAA-C_{60} compared PAA-C_{60}. The peak at 1630 cm^{-1} and shoulder at 1530 cm^{-1} are assigned to NH_3^+ asymmetric deformation, while the band at 1473 cm^{-1} corresponds to NH_3^+ symmetric deformation. The bands at 1570, 1435 and 1385 cm^{-1} are related to the formation of ammonium carbamate pairs and specifically the carbamate ion groups. The time evolution of the spectra of F1-PAA-C_{60} is clearly faster than that of PAA-C_{60} at 90 °C, demonstrating quicker CO_2 sorption kinetics in the former. Clearly, both carbamic acid and ammonium carbamate species are formed upon adsorption of CO_2 in both PAA-C_{60} and F1-PAA-C_{60}, but faster in the fluoroalkyl modified material.

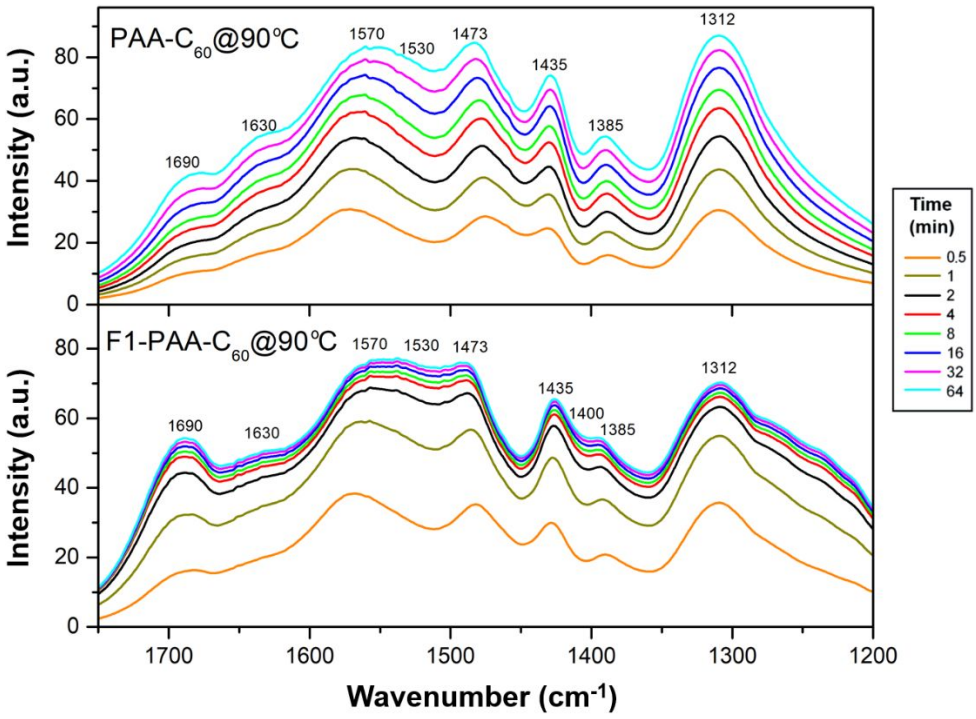

Figure 6. *In-situ* FTIR spectra for CO_2 sorption of PAA-C_{60} and F1-PAA-C_{60} collected overtime in one component pure CO_2 at 90 °C and atmospheric pressure.

Positron Annihilation Lifetime Spectroscopy (PALS)

The effect of GOF on the evolution of free volume elements in cross-linked PAA sorbents was investigated. To this purpose, PALS was applied, which is an experimental method suitably used for the quantitative measurement of the free volume at the nano and mesoscale in molecular matter and polymers (see ESI).[61, 62] The low electron density in void spaces favors the formation of a bond state between an electron and a positron, called positronium (Ps). A direct correlation is found between the size of the free volume and the lifetime of the triplet state, i.e. the ortho-positronium (o-Ps) located in the void. According to the Tao-Eldrup model, the lifetime, τ, of o-Ps in the pick-off processes is a function of the free volume radius, R, which is approximated by a sphere:[63, 64]

$$\tau[ns] = 0.5\left[1 - \frac{R}{R+\Delta} + \frac{1}{2\pi}\sin\left(2\pi\frac{R}{R+\Delta}\right)\right]^{-1} \quad (1)$$

where Δ is the empirical parameter (Δ = 0.1656 nm) describing the depth of penetration of the positron wave function and range of overlap with electrons wavefunctions. This relationship is used in this study for the determination and analysis of the free-volume present in plain and alkylfluorinated PAA-C_{60}.

Three lifetime components were resolved in all measured positron annihilation spectra to obtain a satisfactory χ^2 close to unity (Figure S10, see ESI). The first component was close to 0.2 ns (annihilation of free positrons and/or p-Ps), the second one approached 0.4 ns (due to the annihilation of trapped positrons at molecular defects other than free positron states), but the most interesting one is the longest, the third component, which is associated with the o-Ps formation and annihilation in the free volume. The values, intensities and calculated radii of free volume elements of the third component for both PAA-C_{60} and F1-PAA-C_{60} are summarized in Table 2.

Table 2. The values of the longest lifetime components τ_3 with their intensities I_3 and calculated, according to Eq. 1, radius R of the free volume resolved from the positron lifetime spectra measured for the PAA-C_{60} and F1-PAA-C_{60} samples. Both samples were annealed at 90 °C under Ar atmosphere prior to PALS measurements. Uncertainties are shown in parentheses.

Sample	τ_3 **[ns]**	I_3 **[%]**	R **[nm]**
PAA-C_{60}	1.71(0.04)	5.02(0.30)	0.256(0.004)
F1-PAA-C_{60}	2.10(0.17)	1.76(1.2)	0.294(0.015)

We observed a long lifetime component of about 1.71 ns in PAA-C_{60} and 2.10 ns in F1-PAA-C_{60}, confirming the presence of free volume in the molecular structure with approximate radii of 0.256 nm for PAA-C_{60} and 0.294 nm for F1-PAA-C_{60}. One should also notice the small intensity values of these components, which are about 5.02 % for PAA-C_{60} and 1.76 % for F1-PAA-$C_{60.}$ These low intensities were attributed to the quenching effect of C_{60} molecules on Ps formation, further exacerbated by the additional quenching effect of highly electronegative fluorine. The results show that the fluoroalkyl groups grafted on PAA chains increase the size of the free volume elements. We thus envisage that the incorporation of hydrophobic GOF disrupts the hydrogen bonding and the chain packing within PAA macromolecules, creating additional interchain spacing which effectively acts as extra CO_2 diffusion pathways. This can facilitate the diffusion of CO_2 molecules and enhance the gas transport properties of highly loaded amines at ambient temperature.[10] A similar enhancing effect has been also observed in crosslinked PEI materials, where functionalization with either hydrocarbon or fluorocarbon additives promoted better CO_2 sorption. Introduction of epoxy additives disrupted the hydrogen bonding network, in which amines are involved, and afforded improved uptakes at lower temperature. The steric bulk of the additive is recognized as the pivotal factor for the observed enhancement, with branched hydrocarbon chain exhibiting a more pronounced effect than linear fluorocarbon chain additives.[14]

An increase of radius of about 0.04 nm (ca. 16%) of the free volume elements, while misleadingly minor, is indeed critical to facilitate CO_2 transport and substantially increase the CO_2 sorption properties of the fluorinated sorbents in comparison with their bare counterparts. This is in agreement with work by Song et al. where an increase of radius of

free volume elements of 0.03 to 0.06 nm in polyimide membranes, via the inclusion of ZIF-8 nanoparticles, was instrumental to considerably enhance the gas permeation properties of the membranes.[65] Other authors have observed similar direct correlations between improved gas permeabilities and increased o-Ps lifetimes in polyimide membranes.[66-68]

Conclusions

The functionalization of poly(allylamine) (PAA), an aminopolymer exclusively containing primary amines, with short fluoroalkyl chains, resulted in a drastic change in CO_2 capture performance. The fluoroalkyl-modified PAA sorbent boasted an almost tripled CO_2 uptake capacity and more than quadruple increases amine efficiency at ambient temperature. The fluoroalkyl chains increased the amount of free void volume present in the sorbent, which in turn facilitated the diffusion of CO_2 in the bulk of the polymer. In simulated direct air capture conditions, the fluorinated sorbent achieved a significant CO_2 capture capacity of 1.30 mmol/g, corresponding to 2.28 mmol CO_2 per gram of polymer. These results demonstrate that the inclusion of void volume via the addition of incompatible hydrophobic fluoroalkyl chains in hydrophilic polyamines is a workable approach to enable drastic improvement of carbon capture performance together with impressive amine efficiencies at a lower temperature.

Experimental Section

Materials

Poly(allylamine) hydrochloride (PAH; analytical grade, MW 120,000-180,000 g/mol) was provided by Alfa Aesar. Fullerene C_{60} (99.5%), glycidyl 2,2,3,3,4,4,5,5-octafluoropentyl ether (GOF; 96%), and triethylamine (≥99.5%) were purchased from Sigma Aldrich. Potassium hydroxide (99.98%) was obtained from Acros, while methanol (HPLC, 99.8%)

was purchased from Fischer Scientific. The dialysis tube with a molecular weight cut-off (MWCO) of the 6,000-8,000 g/mol was obtained from Spectrum.

Synthesis

PAA-C_{60}: PAH (0,2 g) was added in small portions to a solution of potassium hydroxide (0.6 g) in methanol (6 mL). The solution was stirred for 48 h at room temperature and subsequently centrifuged to separate the precipitated potassium chloride. The supernatant was dialyzed against methanol to completely remove the excess potassium hydroxide. chloroform (24 mL) was added to the methanolic solution of PAH and mixed afterwards with a C_{60} solution (24 mg in 44 mL of toluene) in the presence of triethylamine (1 mL). A dark grey precipitate was formed and filtered on a 0.45 μm PTFE filter (Chemlab MTF100047H). The PAA-C_{60} precipitate was dried at 80 °C in an oven under air overnight and then collected.

F-PAA-C_{60}: PAH (0,2 g) was added in small portions to a solution of potassium hydroxide (0.6 g) in methanol (6 mL). The solution was stirred for 48 h at room temperature and subsequently centrifuged to separate the precipitated potassium chloride. The supernatant was dialyzed against methanol to completely remove the excess potassium hydroxide. Obtained PAA solution (8 mL) was mixed with 31.6 and 38 μL of GOF, for F1-PAA-C_{60} and F2-PAA-C_{60}, respectively, for 24 h at room temperature. Chloroform (24 mL) was then added to the functionalized PAA solution and afterwards mixed with a C_{60} solution (24 mg in 44 mL of toluene) in the presence of triethylamine (1 mL). A brown/grey precipitate was formed and separated via centrifugation. The F-PAA-C_{60} precipitate was dried overnight at 80 °C in an oven under air and then collected.

Gravimetric determination of PAA content

The content of PAA in the methanolic solution resulted from dialysis was determined gravimetrically. A thermogravimetric analyzer (TA Instruments SDT Q600) was used to heat the sample above methanol boiling point, i.e. 70 °C (1 °C/min), under Argon atmosphere and weigh the residual PAA.

CHN Elemental Analysis

A vario MICRO cube instrument in CHN mode was used for elemental analysis. The samples were initially heated at 110 °C under vacuum to desorb the pre-adsorbed species and then loaded in tin boats. Linear calibrations obtained with acetanilide standard were used for all elements. A ceramic ash crucible/finger was placed into the combustion tube for the analysis of the fluorinated samples.

SEM/EDX

Scanning electron microscopy images were taken using SEM Bench-top TM3030 (Hitachi High-Technology Corporation, Japan). Energy dispersive X-ray spectroscopy was performed using AztecOne system (Oxford Instruments, UK) attached to the SEM, with an accelerating voltage of 5 kV and a count number of 50,000.

Gravimetric CO_2 uptake

A TA Instruments SDT Q600 Thermogravimetric Analysis/Differential Scanning Calorimetry (TGA/DSC) was used for dynamic CO_2 uptake measurements. Capture tests were carried out at atmospheric pressure. Pure CO_2 (99.99%), 10% CO_2 (equilibrated in N_2) and 400 ppm CO_2 (equilibrated in N_2) were used for sorption runs, while pure Ar (99.995%) was used as purging gas for samples activation. In a typical run, 5-8 mg of the sample was loaded in an aluminium sample pan and treated at 90 °C under Ar atmosphere (100 mL/min) to remove all the pre-adsorbed species. The temperature was subsequently

set to sorption temperature, and the gas was then switched to either pure CO_2 or 10% CO_2 or 400 ppm CO_2 (95 mL/min) and held at that temperature until equilibrium (wt.%/min < 0.05). The CO_2 uptake was estimated from the mass gain in the sorption process.

Volumetric CO_2 uptake

CO_2 adsorption isotherms were collected on a Quantachrome iSorbHP1 at 25 and 90 °C and up to 5 bar using approximately 70 mg of the sample. Prior to analysis, the samples were degassed under vacuum on the instrument for 6 h at 90 °C. A sorption rate limit of 0.1 mbar/min was set at each pressure point as equilibrium setting.

Simultaneous volumetric CO_2 adsorption and microcalorimetry

CO_2 adsorption capacities and heats of adsorption were measured using a combined calorimetric−volumetric adsorption apparatus consisting of a Tian-Calvet calorimeter. In a typical experiment, 50 mg of the pelletized (1000 psi, 150−250 μm) sorbent was inserted into one side of the two-pronged sample cell, the other being left empty as a reference. The cell is encased in an aluminium block with highly sensitive thermopiles. The sample was pretreated at 90 °C for 3 h under 15 Pa vacuum before setting to the sorption temperature (30 and 90 °C) and initiating the sorption process. Two pressure transducers connected to the cell and reservoir areas, which were maintained at 30 °C with heating tape, were used to measure the CO_2 uptake. The amount of adsorbed CO_2 was calculated using a mole balance with initial and final pressure values from the cell and reservoir. Heats of CO_2 adsorption were simultaneously recorded while the dosed CO_2 was being adsorbed. When the cell pressure change was less than 0.01 Pa/min, the system was assumed to have reached pseudo equilibrium, signifying the end of the collection for that data point. The CO_2 pressure was incrementally increased to simultaneously generate an adsorption

isotherm and calculate the heat of adsorption. Thus, the reported heats of adsorption are for the incremental amount of CO_2 adsorbed and not an average over all CO_2 adsorbed.

In-situ transmission FTIR spectroscopy

In-situ transmission FTIR spectroscopy: Each sample was pressed into a circular self-supported wafer (2 cm in diameter) and loaded into a sample holder. The *in-situ* IR cell was assembled together with the cell body, sample holder, SrF_2 IR windows, and heating block. The assembled *in situ* IR cell was inserted into a Nicolet 8700 FTIR spectrometer. The sample was activated at 90 °C for 3 h under helium flow (80 mL/min) and cooled to 30 °C, and then a background spectrum was collected before the CO_2 adsorption. All *in-situ* IR spectra of the material during CO_2 adsorption were collected against the background spectrum of the activated sorbents, including the contribution of the cell. Subsequently, the flow was switched from helium to a CO_2 gas stream for 1 h. During this period, a spectrum was recorded every minute. Each spectrum was collected with 32 scans at a resolution of 4 cm^{-1}. After each experiment, a circular stamp (6.35 mm in diameter) was used to cut the wafer, and it was weighed to determine its density. All spectra were normalized by the density of the wafer.

PALS Analysis

A digital positron lifetime spectrometer manufactured by TechnoAP with two photomultipliers: H3378-50 each one coupled with a single crystal of BaF_2 scintillators was used in the current studies. The time resolution (full width half maximum, FWHM) of the instrument was about 190 ps. The positron source used in our experiment was a ^{22}NaCl-solution evaporated on a 7 μm thick Kapton foil with an activity of about 20 μCi. More

than 10^6 counts were collected for each positron lifetime spectrum. All spectra were deconvoluted using LT code,[69] the background and source correction was included.

Conflicts of interest

There are no conflicts to declare.

Acknowledgments

Financial support was provided by the Reduce Industrial Carbon Emissions (RICE) and Flexible Integrated Energy Systems (FLEXIS) research operations part funded by the EU's European Regional Development Fund through the Welsh Government. We also acknowledge support from the SUSTAIN Manufacturing Hub funded by the Engineering and Physical Sciences Research Council (EP/S018107/1). Funding for the work of CJY, JJL and CWJ was provided in part by UNCAGE-ME, an Energy Frontier Research Center funded by the U.S. Department of Energy, Office of Science, Basic Energy Sciences under award no. DE-SC0012577. MT wish to acknowledge funding from the European Union's Horizon 2020 research and innovation programme under the Marie Skłodowska-Curie grant agreement No 663830. JMU-K wish to acknowledge the project 18A12-210FP of the INL Laboratory Directed Research & Development (LDRD) program.

References

1. https://www.esrl.noaa.gov/gmd/ccgg/trends/mlo.html., (accessed March 2021).
2. T. Covert, M. Greenstone and C. R. Knittel, *J. Econ. Perspect.*, 2016, **30**, 117-138.
3. G. T. Rochelle, *Science*, 2009, **325**, 1652-1654.
4. G. T. Rochelle, in *Absorption-Based Post-combustion Capture of Carbon Dioxide*, ed. P. H. M. Feron, Woodhead Publishing, 2016, DOI: https://doi.org/10.1016/B978-0-08-100514-9.00003-2, pp. 35-67.
5. A. B. Rao and E. S. Rubin, *Environmental Science & Technology*, 2002, **36**, 4467-4475.
6. E. S. Sanz-Pérez, C. R. Murdock, S. A. Didas and C. W. Jones, *Chem. Rev.*, 2016, **116**, 11840-11876.

7. E. National Academies of Sciences and Medicine, *Negative Emissions Technologies and Reliable Sequestration: A Research Agenda*, The National Academies Press, Washington, DC, 2019.
8. H. A. Patel, J. Byun and C. T. Yavuz, *ChemSusChem*, 2017, **10**, 1303-1317.
9. M. Bui, C. S. Adjiman, A. Bardow, E. J. Anthony, A. Boston, S. Brown, P. S. Fennell, S. Fuss, A. Galindo, L. A. Hackett, J. P. Hallett, H. J. Herzog, G. Jackson, J. Kemper, S. Krevor, G. C. Maitland, M. Matuszewski, I. S. Metcalfe, C. Petit, G. Puxty, J. Reimer, D. M. Reiner, E. S. Rubin, S. A. Scott, N. Shah, B. Smit, J. P. M. Trusler, P. Webley, J. Wilcox and N. Mac Dowell, *Energy Environ. Sci*, 2018, **11**, 1062-1176.
10. M. Oschatz and M. Antonietti, *Energy Environ. Sci*, 2018, **11**, 57-70.
11. S. A. Didas, S. Choi, W. Chaikittisilp and C. W. Jones, *Acc. Chem. Res.*, 2015, **48**, 2680-2687.
12. J. Yu, Y. Zhai and S. S. C. Chuang, *Ind. Eng. Chem. Res.*, 2018, **57**, 4052-4062.
13. A. Koutsianos, A. R. Barron and E. Andreoli, *J. Phys. Chem. C*, 2017, **121**, 21772-21781.
14. L. B. Hamdy, R. J. Wakeham, M. Taddei, A. R. Barron and E. Andreoli, *Chem. Mater.*, 2019, **31**, 4673-4684.
15. X. Xu, C. Song, J. M. Andresen, B. G. Miller and A. W. Scaroni, *Energy Fuels*, 2002, **16**, 1463-1469.
16. X. Xu, C. Song, J. M. Andrésen, B. G. Miller and A. W. Scaroni, *Microporous Mesoporous Mater.*, 2003, **62**, 29-45.
17. R. S. Franchi, P. J. E. Harlick and A. Sayari, *Ind. Eng. Chem. Res.*, 2005, **44**, 8007-8013.
18. G. P. Knowles, J. V. Graham, S. W. Delaney and A. L. Chaffee, *Fuel Process. Technol.*, 2005, **86**, 1435-1448.
19. T. L. Donaldson and Y. N. Nguyen, *Ind. Eng. Chem. Fundam.*, 1980, **19**, 260-266.
20. W. Xie, M. Yu and R. Wang, *Aerosol Air Qual Res*, 2017, **17**, 2715-2725.
21. E. Andreoli, L. Cullum and A. R. Barron, *Ind. Eng. Chem. Res.*, 2015, **54**, 878-889.
22. X. Feng, G. Hu, X. Hu, G. Xie, Y. Xie, J. Lu and M. Luo, *Ind. Eng. Chem. Res.*, 2013, **52**, 4221-4228.
23. A. Heydari-Gorji, Y. Yang and A. Sayari, *Energy Fuels*, 2011, **25**, 4206-4210.
24. M. Jahandar Lashaki and A. Sayari, *Chem. Eng. J.*, 2018, **334**, 1260-1269.
25. R. Kishor and A. K. Ghoshal, *Ind. Eng. Chem. Res.*, 2017, **56**, 6078-6087.
26. L. Wang, M. Yao, X. Hu, G. Hu, J. Lu, M. Luo and M. Fan, *Appl. Surf. Sci.*, 2015, **324**, 286-292.
27. X. Yan, L. Zhang, Y. Zhang, G. Yang and Z. Yan, *Ind. Eng. Chem. Res.*, 2011, **50**, 3220-3226.
28. H. Zhang, A. Goeppert, S. Kar and G. K. S. Prakash, *J. CO2 Util.*, 2018, **26**, 246-253.
29. H. T. Kwon, M. A. Sakwa-Novak, S. H. Pang, A. R. Sujan, E. W. Ping and C. W. Jones, *Chem. Mater.*, 2019, **31**, 5229-5237.
30. Y. Kuwahara, D.-Y. Kang, J. R. Copeland, N. A. Brunelli, S. A. Didas, P. Bollini, C. Sievers, T. Kamegawa, H. Yamashita and C. W. Jones, *J. Am. Chem. Soc.*, 2012, **134**, 10757-10760.
31. J. Liu, D. Cheng, Y. Liu and Z. Wu, *Energy Fuels*, 2013, **27**, 5416-5422.

32. A. A. Rownaghi, A. Kant, X. Li, H. Thakkar, A. Hajari, Y. He, P. J. Brennan, H. Hosseini, W. J. Koros and F. Rezaei, *ChemSusChem*, 2016, **9**, 1166-1177.
33. M. A. Sakwa-Novak, A. Holewinski, C. B. Hoyt, C.-J. Yoo, S.-H. Chai, S. Dai and C. W. Jones, *Langmuir*, 2015, **31**, 9356-9365.
34. M. E. Potter, K. M. Cho, J. J. Lee and C. W. Jones, *ChemSusChem*, 2017, **10**, 2192-2201.
35. A. Holewinski, M. A. Sakwa-Novak and C. W. Jones, *J. Am. Chem. Soc.*, 2015, **137**, 11749-11759.
36. A. Heydari-Gorji, Y. Belmabkhout and A. Sayari, *Langmuir*, 2011, **27**, 12411-12416.
37. A. Sayari, Q. Liu and P. Mishra, *ChemSusChem*, 2016, **9**, 2796-2803.
38. E. Andreoli and A. R. Barron *ChemSusChem*, 2015, **8**, 2635-2644.
39. P. Sharma, S. Chakrabarty, S. Roy and R. Kumar, *Langmuir*, 2018, **34**, 5138-5148.
40. M. A. Sakwa-Novak, S. Tan and C. W. Jones, *ACS Appl. Mater. Interfaces*, 2015, **7**, 24748-24759.
41. J. Wang, H. Huang, M. Wang, L. Yao, W. Qiao, D. Long and L. Ling, *Ind. Eng. Chem. Res.*, 2015, **54**, 5319-5327.
42. J. Wang, M. Wang, B. Zhao, W. Qiao, D. Long and L. Ling, *Ind. Eng. Chem. Res.*, 2013, **52**, 5437-5444.
43. A. Goeppert, H. Zhang, R. Sen, H. Dang and G. K. S. Prakash, *ChemSusChem*, 2019, **12**, 1712-1723.
44. D. A. Long, *J. Raman Spectrosc.*, 2004, **35**, 905-905.
45. E. Andreoli, E. P. Dillon, L. Cullum, L. B. Alemany and A. R. Barron, *Sci. Rep.*, 2014, **4**, 7304.
46. M. Caplow, *J. Am. Chem. Soc.*, 1968, **90**, 6795-6803.
47. S. J. Park, J. J. Lee, C. B. Hoyt, D. R. Kumar and C. W. Jones, *Adsorption*, 2020, **26**, 89-101.
48. C. Gebald, J. A. Wurzbacher, P. Tingaut, T. Zimmermann and A. Steinfeld, *Environmental Science & Technology*, 2011, **45**, 9101-9108.
49. L. Wang and R. T. Yang, *J. Phys. Chem. C*, 2011, **115**, 21264-21272.
50. M. E. Potter, S. H. Pang and C. W. Jones, *Langmuir*, 2017, **33**, 117-124.
51. M. A. Alkhabbaz, P. Bollini, G. S. Foo, C. Sievers and C. W. Jones, *J. Am. Chem. Soc.*, 2014, **136**, 13170-13173.
52. S. A. Didas, A. R. Kulkarni, D. S. Sholl and C. W. Jones, *ChemSusChem*, 2012, **5**, 2058-2064.
53. A. Samanta, A. Zhao, G. K. H. Shimizu, P. Sarkar and R. Gupta, *Ind. Eng. Chem. Res.*, 2012, **51**, 1438-1463.
54. M. R. Mello, D. Phanon, G. Q. Silveira, P. L. Llewellyn and C. M. Ronconi, *Microporous Mesoporous Mater.*, 2011, **143**, 174-179.
55. S. J. Thompson, M. Soukri and M. Lail, *Chem. Eng. J.*, 2018, **350**, 1056-1065.
56. Y. Belmabkhout and A. Sayari, *Adsorption*, 2009, **15**, 318-328.
57. R. Serna-Guerrero, Y. Belmabkhout and A. Sayari, *Chem. Eng. J.*, 2010, **161**, 173-181.
58. Z. Bacsik, N. Ahlsten, A. Ziadi, G. Zhao, A. E. Garcia-Bennett, B. Martín-Matute and N. Hedin, *Langmuir*, 2011, **27**, 11118-11128.

59. G. S. Foo, J. J. Lee, C.-H. Chen, S. E. Hayes, C. Sievers and C. W. Jones, *ChemSusChem*, 2017, **10**, 266-276.
60. C.-J. Yoo, L.-C. Lee and C. W. Jones, *Langmuir*, 2015, **31**, 13350-13360.
61. G. Consolati and F. Quasso, 2010, DOI: 10.1002/9780470600160.ch10, pp. 391-419.
62. G. Dlubek, 2010, DOI: 10.1002/9780470600160.ch11, pp. 421-472.
63. S. J. Tao, *The Journal of Chemical Physics*, 1972, **56**, 5499-5510.
64. M. Eldrup, D. Lightbody and J. N. Sherwood, *Chem. Phys.*, 1981, **63**, 51-58.
65. Q. Song, S. K. Nataraj, M. V. Roussenova, J. C. Tan, D. J. Hughes, W. Li, P. Bourgoin, M. A. Alam, A. K. Cheetham, S. A. Al-Muhtaseb and E. Sivaniah, *Energy Environ. Sci*, 2012, **5**, 8359-8369.
66. K. Tanaka, T. Kawai, H. Kita, K.-i. Okamoto and Y. Ito, *Macromolecules*, 2000, **33**, 5513-5517.
67. A. Shimazu, T. Miyazaki, S. Katayama and Y. Ito, *J. Polym. Sci., Part B: Polym. Phys.*, 2003, **41**, 308-318.
68. J. Kruse, J. Kanzow, K. Rätzke, F. Faupel, M. Heuchel, J. Frahn and D. Hofmann, *Macromolecules*, 2005, **38**, 9638-9643.
69. J. Kansy, LT programs, http://prac.us.edu.pl/kansy/index.php?id¼lt10, (accessed 16 November 2010).